S10. EXTREME RAINFALL IN THE UNITED KINGDOM DURING WINTER 2013/2014: THE ROLE OF ATMOSPHERIC CIRCULATION AND CLIMATE CHANGE

Nikolaos Christidis and Peter A. Stott

This document is a supplement to "Extreme Rainfall in the United Kingdom During Winter 2013/2014: The Role of Atmospheric Circulation and Climate Change," by Nikolaos Christidis and Peter A. Stott (*Bull. Amer. Meteor. Soc.*, **96** (12), S46–S50) • DOI:10.1175/BAMS-D-15-00094.1

CMIP5 models and experiments. The seven CMIP5 models used in this study are listed in Table S10.1. The models provide data from simulations with all historical forcings (ALL) and natural forcings only (NAT) that end in year 2012. Each model contributed several simulations per experiment. In total there are 43 and 33 simulations with and without anthropogenic forcings, respectively. The effect of internal climate variability is minimal in the mean of the simulations as illustrated in the first figure of our paper (see Fig. 10.1). Monthly rainfall data are used to estimate the total December–February (DJF) U.K. rainfall over period 1900–2012 and daily data were used to compute the R10x index in the U.K. region over period 1948–2012. Two of the models (GISS-E2-H and GISS-E2-R) do not provide daily precipitation data and hence fewer simulations were used to compute R10x (33 and 23 with ALL and NAT forcings, respectively).

By extracting the last 20 years of the ALL and NAT simulations, we create ensembles of U.K. rainfall representative of winters in recent years. We further partition modelled winters between those that correlate well with the 500-hPa anomaly in 2013/14 (correlation coefficient greater than 0.6) and those with lower correlations. The ensemble sizes created by this grouping are shown in Table S10.2. The rarity of the 2014/15 event implies that the likelihood of exceeding the observed rainfall amount cannot be accurately estimated using our relatively small ensembles. We therefore employ the more moderate threshold of a 1-in-10 year event, which is useful for adaptation planning and commonly used in attribution studies.

Table S10.1. CMIP5 models used in the study and number of simulations in experiments with and without anthropogenic forcings.

Model	ALL	NAT
HadGEM2-ES	4	4
CanESM2	5	5
CNRM-CM5	10	6
CSIRO-Mk3.6.0	10	5
GISS-E2-H	5	5
GISS-E2-R	5	5
IPSL-CM5A-LR	4	3
Total	**43**	**33**

Table S10.2. Number of estimates of DJF rainfall and R10x from simulated winters in years 1993–2012. The table gives the total number of winters as well as the cases with high and low correlations to the 2013/14 circulation.

	DJF	R10x
ALL (total)	860	660
ALL (high corr.)	175	142
ALL (low corr.)	685	518
NAT (total)	660	460
NAT (high corr.)	166	109
NAT (low corr.)	494	351

Simulated patterns of the atmospheric circulation. The mean 500-hPa geopotential height and wind fields in the North Atlantic region estimated with NCEP/NCAR reanalysis data and averaged over the boreal winter months and the climatological period of 1961–90 are illustrated in Fig. S10.1a. The

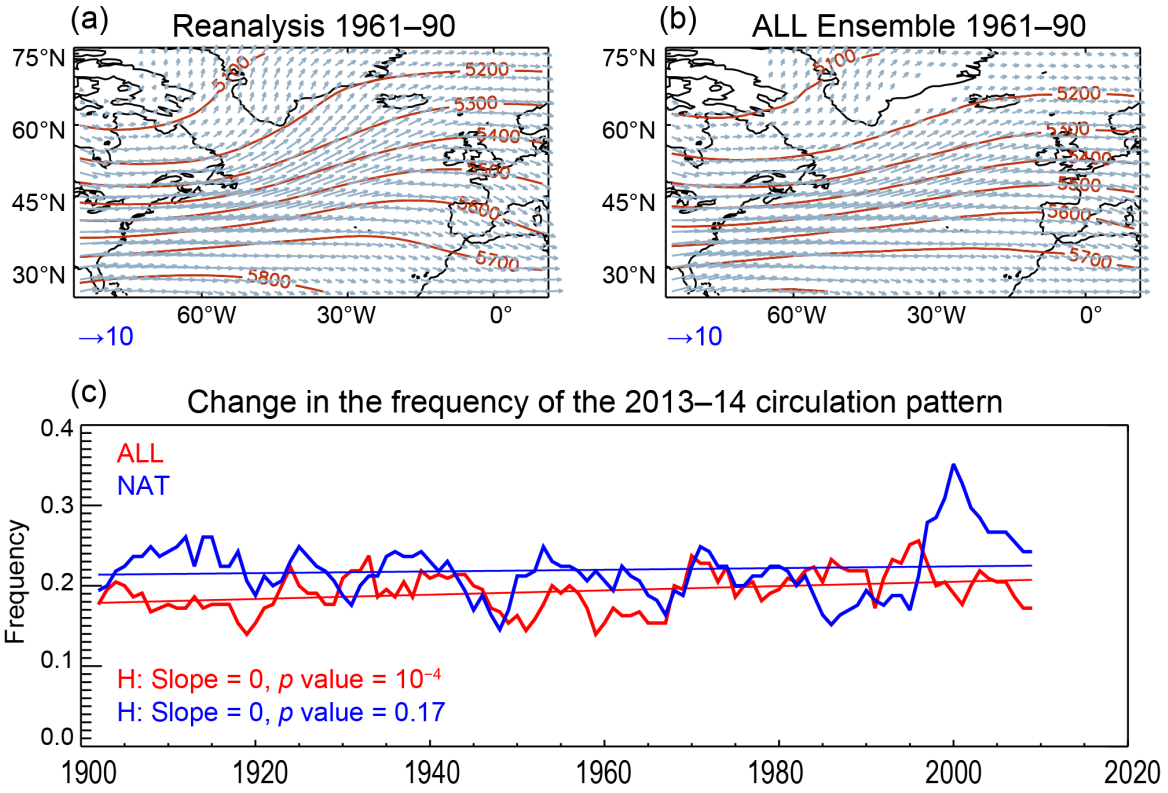

Fig. S10.1. Modelled circulation patterns. (a) Map of the 500-hPa height (red contours, m) and wind (blue vectors, m s^{-1}) in the North Atlantic during 1961–90 based on data from the NCEP/NCAR reanalysis. (b) As in (a), but for the mean of the ALL simulations. (c) Timeseries of the frequency of winter circulation patterns similar to 2013/14 from experiments with (red) and without (blue) anthropogenic forcings. The *p*-values refer to testing of the hypothesis that the least square fit has a zero trend.

ensemble mean of the 43 simulations with all forcings produces very similar flow patterns over the same period (Fig. S10.1b). Moreover, as shown in the first figure of our paper (Fig. 10.1), the high correlation cases from the ALL experiment display flow anomalies relative to the climatological mean that are similar to the characteristic pattern of 2013/14.

We next use model simulations to examine whether the frequency of the 2013/14 pattern has been changing in recent decades. Figure S10.1c shows timeseries of the frequency since 1900 estimated from ALL and NAT simulations. Using 5-year running means, we compute the frequency as the number of winters in each 5-year window that resemble DJF 2013/14 per total number of winters from all the model simulations in the same time window. The timeseries suggest that longer records would be required to robustly identify any long-term change due to high interdecadal variability. However, testing the hypothesis that the least-square fit has a zero slope indicates that for the experiment that includes anthropogenic forcings, the trend in the frequency of the characteristic circulation pattern of 2013/14 is significantly different from zero. A model study by Hoerling et al. (2012) also finds evidence that oceanic warming may favour a south-westerly winter flow over the United Kingdom similar to the 2013/14 pattern. The peak in year 2000 in the NAT timeseries is most likely a manifestation of internal climate variability, given the absence of major volcanic eruptions, or pronounced solar activity in the early 2000s.

Model evaluation. Model evaluation is an essential part of any attribution study, helping to establish whether the models used in the analysis are fit for purpose. We carry out our evaluation assessment using NCEP/NCAR reanalysis data because of the better coverage over the U.K. region compared to the HadUKP observations. Comparisons between rainfall anomaly timeseries from observations and reanalysis data show a good agreement between the two datasets in the representation of the year-to-year variations for both DJF rainfall and R10x (correlation coefficients 0.95 and 0.75 respectively). The HadUKP timeseries display higher variability, as would be expected, given the smaller observational coverage compared to the full coverage of the reanalysis.

Rainfall distributions over period 1948–2011 obtained with data from our multi-model (ALL) ensemble are found to be in good agreement with the distributions from reanalysis data (Figs. S10.2a,b). The agreement is better for DJF precipitation and remains good when models are tested individually. The *p*-values from Kolmogorov–Smirnov tests that compare the reanalysis distribution with the distribution from the multi-model ensemble and individual models are shown in Figs. S10.2c,d. The lower *p*-values for R10x imply a lower level of agreement. When the CanESM2 model is tested individually, the hypothesis that the modelled R10x distribution is indistinguishable from the reanalysis fails at the 5% significant level, whereas the CNRM-CM5 model passes the test only marginally. Nevertheless, comparisons with individual simulations of these models pass the test and larger ensembles would therefore be required to establish how well they reproduce the R10x distribution.

Looking at the tails of the seasonal and R10x distributions we also find that the modelled return times of more extreme events are consistent with the reanalysis (Figs. S10.2ef). We examine events with return times of up to several decades and find that the multimodel ensemble is generally in good agreement with the reanalysis. For both DJF rainfall and R10x, the multimodel ensemble yields moderately higher return times as the return level increases, but the overall level of agreement is considered to be adequate for the purpose of our study.

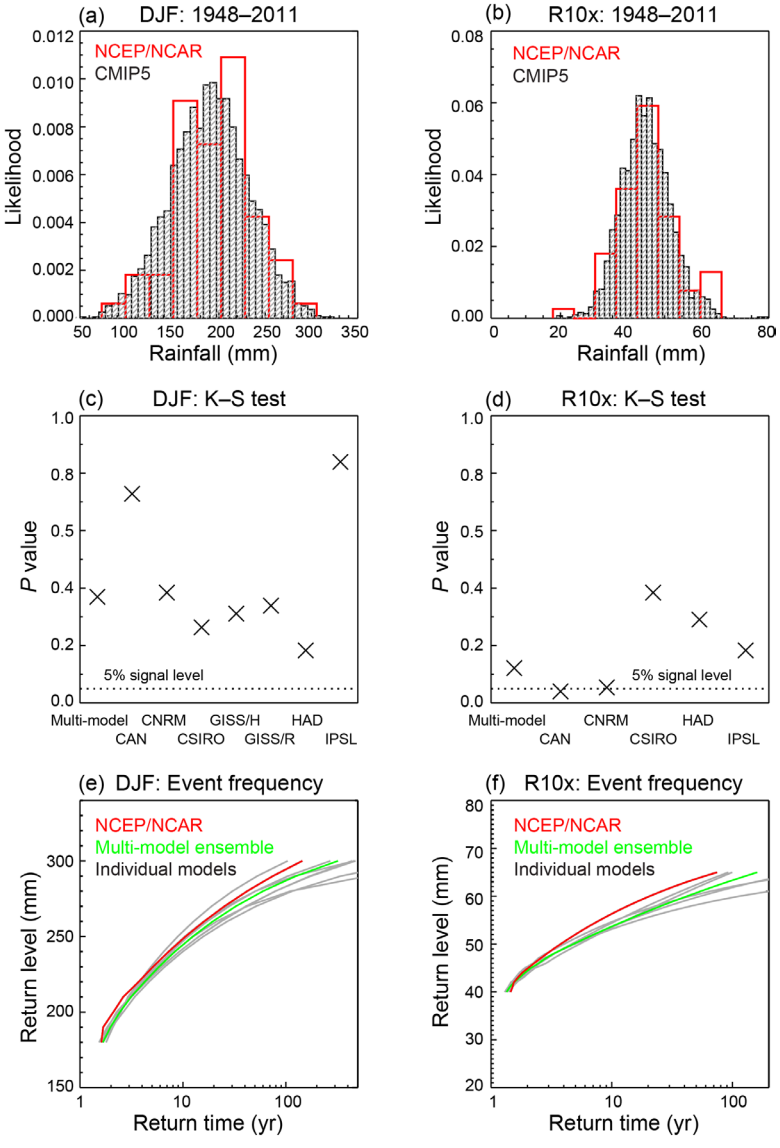

Fig. S10.2. Model evaluation assessment. (a) Normalised distributions of the DJF rainfall in the U.K. region during 1948–2011 estimated with reanalysis data (red) and the ALL multimodel ensemble (gray). (b) As in (a), but for R10x. (c) *p*-values of Kolmogorov–Smirnov tests that assess whether modelled DJF distributions are distinguishable from the reanalysis. Values above the dotted line suggest the distributions are not distinguishable when tested at the 5% significance level. (d) The *p*-values for distributions of R10x. (e) Return level of DJF rainfall in the United Kingdom plotted against the return time. Estimates of the return time were obtained with the generalised Pareto distribution for levels that lies in the tails of the distributions. Results are shown for the NCEP/NCAR reanalysis (red), the multi-model ensemble (green) and individual models (gray). (f) As in (e), but for R10x.

Probabilities and uncertainties. We estimate the probabilities of U.K. rainfall exceeding the amount associated with a 1-in-10 years event using the generalised Pareto distribution if the threshold lies at the tail of the distribution. Changes in the likelihood are reported as the ratio of the probabilities of extreme rainfall 1) for winters with high and low correlation flow patterns relative to winter 2013/14, and 2) with and without the effect of human influence under conditions similar to 2013/14. We employ a Monte Carlo procedure to estimate uncertainties in the probability change as in previous work (e.g., Christidis et al. 2013). For example, in order to investigate the effect of human influence, we compute the probabilities of exceeding the extreme rainfall threshold based on

Table S10.3. Probability ratios estimated from simulations of 5 models (as in the main analysis) and 3 models only. The best estimate (50th percentile) of the ratio is reported together with the 5%–95% uncertainty range (in brackets).		
	Estimates from 5 models (HadGEM2-ES, CanESM2, CNRM, CSIRO, IPSL)	**Estimates from 3 models (HadGEM2-ES, CSIRO, IPSL)**
Prob (High)/ Prob(Low)	3.4 (1.5–6.0)	2.6 (0.7–5.1)
Prob (ALL)/ Prob(NAT)	7.5 (2.3–open ended)	4.8 (0.6–open ended)

the ALL and NAT high correlation ensembles (P_{ALL} and P_{NAT}) and obtain the ratio P_{ALL}/P_{NAT}. We then resample the modelled rainfall estimates of the two ensembles, get a new estimate of the probability ratio and repeat the procedure 10 000 times. This gives 10 000 estimates of P_{ALL}/P_{NAT} from which we quantify the 5%–95% uncertainty range. When assessing the anthropogenic effect we find that PNAT may become near-zero, which leads to an open ended uncertainty range (e.g., main text Fig. 10.2f).

A sensitivity test. We repeated our analysis for R10x after removing simulations of the two models (CanESM2 and CNRM-CM5) that give the poorest agreement with the reanalysis on the climatological distribution of R10x (Fig. S10.2d). The change in the probability of extreme R10x events under the influence of the 2013/14 circulation flow and anthropogenic forcings is reported in Table S10.3 for the different model combinations. The analysis with the 3 models gives probability ratios of the same order as our original analysis and does not qualitatively change the main conclusions of our work. We therefore retain all models in our main analysis, as larger samples are deemed more suitable for studies of rare events.

REFERENCES:

Christidis, N., P. A. Stott, A. Scaife, A. Arribas, G. S. Jones, D. Copsey, J. R. Knight, and W. J. Tennant, 2013: A new HadGEM3-A based system for attribution of weather and climate-related extreme events. *J. Climate*, **26**, 2756–2783, doi:10.1175/JCLI-D-12-00169.1.

Hoerling, M., J. Eischeid, J. Perlwitz, X. Quan, T. Zhang, and P. Pegion, 2012: On the increased frequency of Mediterranean drought. *J. Climate*, **25**, 2146–2161, doi:10.1175/JCLI-D-11-00296.1.